Journal of Catalysis **190,** 240–246 (2000)
doi:10.1006/jcat.1999.2728, available online at http://www.idealibrary.com on IDEAL®

On the Origin of the Selectivity of Oxygen Reduction of Ruthenium-Containing Electrocatalysts in Methanol-Containing Electrolyte

N. Alonso-Vante,[1] P. Bogdanoff, and H. Tributsch

Hahn-Meitner-Institut, Dept. Solare Energetik, Glienicker Strasse 100, D-14109 Berlin, Germany
E-mail: alonso@campus.univ-poitiers.fr

Received May 21, 1999; revised October 7, 1999; accepted October 8, 1999

The reactivity with water and methanol of oxygen-reducing ($Ru_{1-x}Mo_xSeO_z$) and oxygen (from water)-evolving eletrocatalysts (RuS_2, RuO_2), which permit electron transfer via ruthenium d-states, was studied using electrochemical techniques and differential electrochemical mass spectroscopy (DEMS). In contrast to platinum, which is depolarised by methanol, ruthenium compounds show a high reactivity with water species and an extremely low reactivity with methanol. We conclude that the ruthenium-centred coordination chemical reactivity with water channels electrochemical currents, thus producing kinetic selectivity. The reason for the higher reactivity with water of Ru d-states as compared to platinum is seen in the higher density of d-states near the Fermi level as shown by this comparative study.

Key Words: **clusters; ruthenium; methanol oxidation; oxygen reduction; selectivity.**

1. INTRODUCTION

Traditional strategies for the development of direct methanol fuel cells (DMFC) concentrate on the development of efficient oxygen reduction and methanol oxidation electrodes, while separating them with solid electrolyte semipermeable membranes (1, 2). This construction involves a quite expensive membrane technology. Furthermore, there is always the risk that membrane degradation may interfere with the operation of the fuel cell (3, 4). An alternative would be to use an oxygen reduction electrode, which is not depolarised by methanol. Such electrodes, which are selectively catalytic, have been developed, $Mo_4Ru_2Se_8$ Chevrel phases (5–8) and $Ru_{1-x}Mo_xSeO_z$ transition metal cluster catalysts (8–10). In order to further develop their interesting property of catalytic selectivity it is necessary to understand the underlying chemical and electrochemical principles. The aim of this work is thus to investigate the physical–chemical nature of the methanol insensitivity of ruthenium-based electrocatalysts.

This study is a continuation of research performed with transition metal compounds, which enable metal-centred interfacial coordination chemical reactions (11). The experience gained with the transition metal disulphides crystallising in the pyrite structure (FeS_2) has shown that the electron transfer mediated via transition metal surface atoms is very efficient. It suppresses the corrosion provided the electron donors can be engaged in coordination type interfacial processes (inner-sphere electron transfer) with the metal centre (12). Such electron donors are I^-, Br^-, Cl^-, OH^-. When, on the other hand, electron donors like Fe^{2+} or iron complexes are active, they cannot engage in interfacial coordination chemical mechanisms and can, therefore, only be involved in outer-sphere electron transfer processes via tunnelling. It could be shown that the quantum efficiency reached in photo processes is, in this case, clearly low and that there is a significant rate of corrosion of the electrode which occurs as a parallel reaction (13). Furthermore, it was shown that coordination type inner-sphere electron transfer (which occurs via the metal centres) and outer-sphere electron transfer occur on different surface sites (12). This has been demonstrated by selectively inhibiting outer-sphere electron transfer through adsorbed organic molecules or very small amounts of platinum (14). These results show that very different rates and kinetic efficiencies for different electron-donating species may be observed at the same electrode interface. For the theoretical calculation of electron transfer, this means that it is not sufficient to take into account the distribution of electronic states in the electrode surface and in the electrolyte. But it is also necessary to specify the location of the electron transfer where chemical interaction with the electron donor may or may not occur.

The ruthenium compounds, which will be comparatively investigated in this publication, are all able to transfer electrons via ruthenium-centred mechanisms. However, transfer will only occur via this mechanism provided the

[1] Present address: Lab. Electrocatalysis, UMR-CNRS 6503, Université de Poitiers, F-86022 Poitiers, France.

0021-9517/00 $35.00

electron donor can be engaged in coordination type interfacial reactions. By comparing different ruthenium-containing catalysts, which facilitate oxygen reduction or oxygen evolution from water, and by comparing their properties with those of platinum electrodes, it will be attempted to specify and understand the reason for the selectivity and insensitivity against methanol oxidation.

2. EXPERIMENTAL

Synthesis and Electrode Preparation

Powder or thin layers (thickness $<0.5\ \mu$m) of Mo–Ru–Se catalysts were synthesised by reaction for 20 h (140°C), under argon atmosphere, molybdenum hexacarbonyl (>99%, Merck), tris-ruthenium dodecacarbonyl (95%, Alpha), and selenium (powder 200 mesh, Alpha), previously dissolved in 100 ml dried-xylene (using a molecular sieve), b.p. 140°C, (Merck No. 8687.1000) under stirring and refluxing conditions. A detailed description of the catalyst synthesis and analysis is given elsewhere (9).

Single crystals of *n*-RuS_2 were grown in our laboratory by chemical vapour transport with bismuth at a temperature gradient of 700–1080°C. $RuTe_2$ was also grown by chemical vapour transport with tellurium at a temperature gradient of 700–1110°C. All crystals were cleaned in aqua regia and then rinsed a few times with deionized water. Thereafter, silver glue was used to make ohmic contact on one side of the crystals. The semiconductors were further insulated using epoxy resin (Scotchcast 3M). The surfaces of the electrodes were used as grown. They were electrochemically activated by making various scans until a defined capacitive current was attained in the base electrolyte.

RuO_2 electrodes were prepared from thin layers (ca. 2000 Å thickness) deposited on titanium substrates. They were prepared by reactive sputtering as described elsewhere (15).

For the differential electrochemical mass spectroscopy (DEMS) the electrodes were prepared from $Ru_{1-x}Mo_xSeO_z$ and RuO_2 powders mixed with Nafion (Dupont, 0.3% in ethanol) and were deposited (about 1 μL) onto glassy carbon (GC) disk substrates (dia. 3 mm). RuO_2 was purchased from Johnson Matthey, alpha products. The quality of this commercial powder was verified by X-ray measurements. The GC substrates were previously polished and washed in an ultrasonic bath. Thereafter, the RuO_2/Nafion and $Ru_{1-x}Mo_xSeO_z$/Nafion layers were dried in a furnace (80°C) to remove residual ethanol. A platinum blade polished and cleaned with water in an ultrasonic bath prior to each measurement was used for DEMS. The geometric surface of all electrodes was of ca. 0.03 cm^2.

Electrochemical Measurements

A standard electrochemical (EG&G Mod. 273) computer-based setup was used for current–potential measurements. The Pyrex cell, having a three-electrode configuration, consisted of two compartments for the working and counter electrodes connected through a porous glass fritt. Platinum and mercury sulphate electrodes (mse), Hg/Hg_2SO_4, 0.5 M H_2SO_4 (mse = 0.65V/nhe), were used as counter and reference electrodes, respectively. All potentials were referred to nhe. The base electrolyte employed was 0.5M H_2SO_4 (pH 0.3) (Merck). Before carrying out an experiment the solutions were purged with argon.

In order to detect the oxygen mass signal (m/e = 32) with DEMS, deuterated methanol (CD_3OD, deuteration degree 99.5%, Merck) was employed (m/e = 36) due to the strong background of normal methanol CH_3OH (m/e = 32). In test measurements and in the frame of our detection sensitivity, the electrooxidation at Pt electrodes with deuterated methanol showed the same reactivity as with normal methanol.

The differential electrochemical mass spectroscopy (DEMS) setup was described elsewhere (16). The measurements were carried out in a special electrochemical cell provided with a three-electrode configuration which allows the detection of volatile products formed at a solid massif working electrode and/or on layers deposited onto the massif glassy carbon (GC) substrates. A detailed description of this cell is described in Ref. (17).

3. RESULTS

Oxygen Reduction Selectivity on $Ru_{1-x}Mo_xSeO_z$ and Pt

The electrocatalytic current as a function of the applied electrode potential of the molecular oxygen reduction in oxygen-saturated 0.5 M H_2SO_4 on the novel powder material $Ru_{1-x}Mo_xSeO_z$, embedded in a Nafion film deposited on a GC disk, is shown in Fig. 1; it is shown on a platinum disk in Fig. 2.

The detected mass signal of oxygen (m/e = 32) is proportional to the concentration of oxygen at the working electrode surface. This concentration is given by the rate of incoming transport of oxygen to the electrode surface, its electrochemical consumption (reduction to water), and the amount of oxygen transferred into the vacuum system of the mass spectrometer. The rate of oxygen transport is sensitively influenced by the geometrical position of the oxygen bubbler near the working electrode. Computer simulations of the mass signal of oxygen clearly indicate that a high gas transport rate (excess concentration of oxygen at the inlet system of the mass spectrometer) shifts the onset potential of the mass signal to more negative potentials in comparison to the onset potential of the faradic current. This is clearly observed in the case of the $Ru_{1-x}Mo_xSeO_z$ system (Fig. 1). Here at an electrocatalytic current of -2 mA/cm^2 no significant oxygen consumption difference in the mass signal,

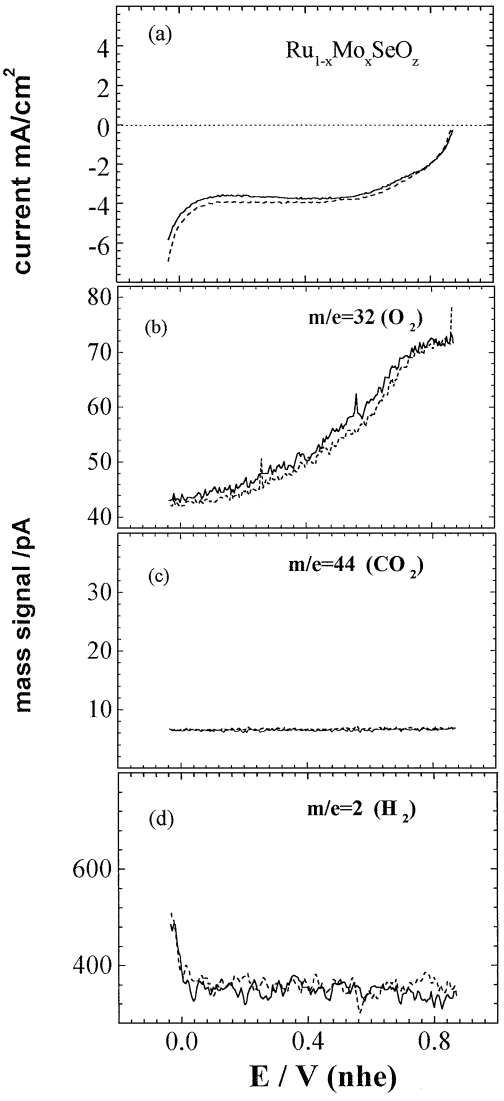

FIG. 1. (a) Current–potential and (b–d) mass signals–potential characteristics of molecular oxygen reduction on $Ru_{1-x}Mo_xSeO_z$ in oxygen-saturated 0.5 M H_2SO_4 (solid lines) and in the presence of 1 M CD_3OD (dashed lines). The mass signals (m/e = 32), (m/e = 44), and (m/e = 2) were measured simultaneously. Scanning was from positive to negative potentials at a rate of 5 mV/s.

in an interval of 60 mV negative from the onset potential (0.86V/nhe), is detected. When working with gases (with the use of a bubbler), as in the case of platinum, the lower transport rate of oxygen produces lower currents with a correct onset of the oxygen mass signal. For a direct comparison of the measurements it is necessary to keep the position of the oxygen bubbler unchanged (geometrical parameters). This problem is overcome when adding liquid chemicals (like methanol) to the electrolyte without varying the geometry of the electrochemical cell.

One key question regarding the electrocatalyst selectivity is the reduction of molecular oxygen in the presence of methanol. This *in situ* confirmation is furnished by DEMS. In fact, the addition of 1 M CD_3OD to 0.5 M H_2SO_4 perturbs neither the current–potential characteristics of the novel $Ru_{1-x}Mo_xSeO_z$ system nor the oxygen consumption mass signal. Furthermore, there is a complete absence, within the experimental sensitivity of our apparatus, of oxidation products of methanol, e.g., carbon dioxide (m/e = 44) in the explored potential range. On the other hand, as is well known, platinum oxidises methanol (see Fig. 2) to CO_2 (18–20). Interestingly, in spite of the methanol oxidation on platinum, its oxygen consumption remains the same. This puts forth evidence for the possibility that this faradic process is occurring in parallel at different sites on the electrode surface.

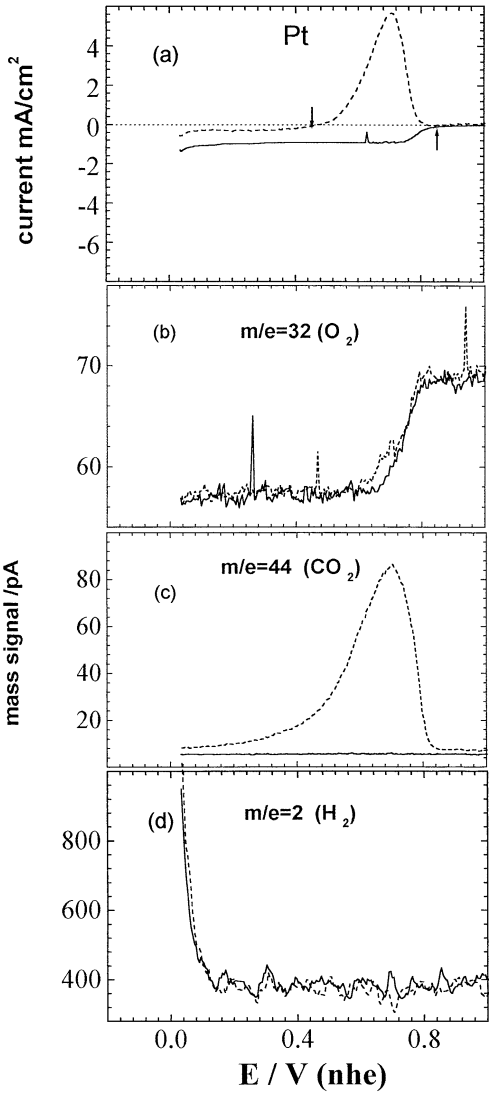

FIG. 2. (a) Current–potential and (b–d) mass signals–potential characteristics of molecular oxygen reduction on platinum in oxygen-saturated 0.5 M H_2SO_4 (solid lines) and in the presence of 1 M CD_3OD (dashed lines). The mass signals (m/e = 32), (m/e = 44), and (m/e = 2) were measured simultaneously. Scanning was from positive to negative potentials at a rate of 5 mV/s.

The overall electrochemical process, that is, the combination of oxygen reduction and methanol oxidation, leads to the formation of a mixed electrode potential which has a negative consequence on the performance of the cell voltage, as observed from the current–potential curve, Fig. 2. There is a shift of ca. −0.41 V from the onset potential (see arrows in the figure). Unlike the consumption of molecular oxygen, the mass signals of the products being formed at the interface show a similar characteristic in comparison to the current-potential curve. Under the same experimental conditions the mass signal of H_2 (m/e = 2) was also recorded simultaneously by DEMS, as contrasted in Figs. 1 and 2. The data presented in Fig. 1 confirm the results reported recently (21).

In order to gain more insight into the selectivity property of the novel compound, we decided to analyse the electrochemical activity of a family of ruthenium-containing compounds with respect to methanol oxidation.

Water and Methanol Oxidation on Ruthenium-Containing Compounds

Figure 3 shows a series of steady-state current–potential curves, in semilogaritmic scales (Tafel plots), obtained from metallic RuO_2 and semiconducting *n*-RuS_2 and *n*-$RuTe_2$ electrodes. Due to their degenerate character, small photoeffects are observed in these ruthenium dichalcogenide samples. One clearly observes that oxygen evolution proceeds easily on RuO_2, followed by RuS_2 (as shown below by DEMS for RuO_2), although one can recognise that the onset oxidation potential on both materials is almost the same (ca. 1.2 V/nhe). The higher slope of RuS_2 reflects the semiconducting character of the material. At applied electrode potentials higher than 1.5 V for RuO_2 and 1.65 V for RuS_2 a change of slope is observed which has been attributed to a change of mechanism, i.e., a corrosion process (22). Furthermore, the anodic behaviour of $RuTe_2$ is mainly due to corrosion. $RuTe_2$ is kinetically much less stable than RuS_2, due to a low contribution (10–20%) of d-states to the valence band, as demonstrated several years ago (23). It is well known that platinum presents a higher overvoltage (0.25V more positive with respect to RuO_2) for oxygen evolution, as shown in Fig. 4. This preliminary comparison puts forth evidence of different degrees of interaction of water with the metallic centres on these various compounds.

A very distinct behaviour in comparison with platinum is observed when methanol is added to the electrolyte. RuO_2 and RuS_2 are bad electrocatalysts for methanol oxidation, and on $RuTe_2$ the recorded current in methanol simply coincides with the curve without methanol, indicating that the main reaction channel is the corrosion process. Independent of the electronic properties of RuO_2 and RuS_2 materials, methanol oxidation sets in at the same potential, i.e., 1.1 V/nhe. At higher applied electrode potentials one observes that methanol oxidation is a competitive reaction with water oxidation. This point will be clarified below. The oxidation of methanol on platinum occurs ca. 0.5 V more negatively than on RuO_2 at $i = 10^{-2}$ mA cm^{-2}. As detected by DEMS, the major product measured in the potential span (0.5 to 1.8 V) was CO_2. It is also recognised that at potentials higher than 1.5 V/nhe water oxidation is strongly diminished in favour of methanol oxidation. This speaks for a complicated potential-dependent mechanism of competition between methanol oxidation and water oxidation on Pt electrodes.

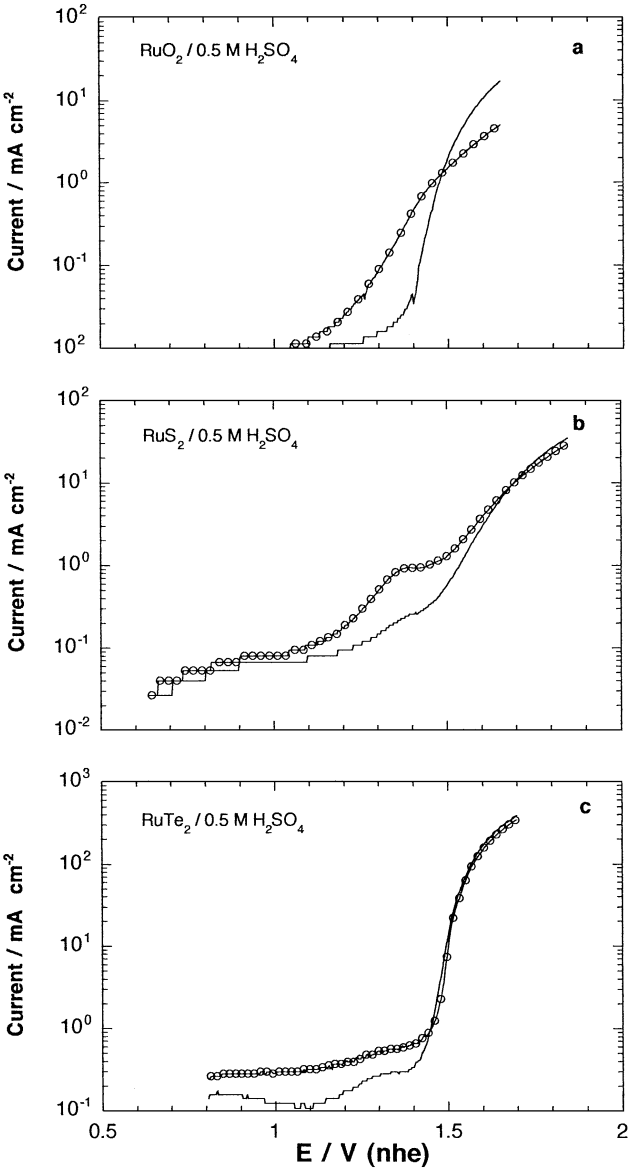

FIG. 3. Current–potential semilogaritmic plots for water oxidation (solid lines) and CH_3OH (1 M) oxidation (open circles) in 0.5 M H_2SO_4 on (a) RuO_2, (b) RuS_2, and (c) $RuTe_2$ electrodes. Scanning was from negative to positive potentials at a rate of 5 mV/s.

This competitive water and methanol oxidation is depicted in Fig. 5 with DEMS for the RuO_2 electrode material

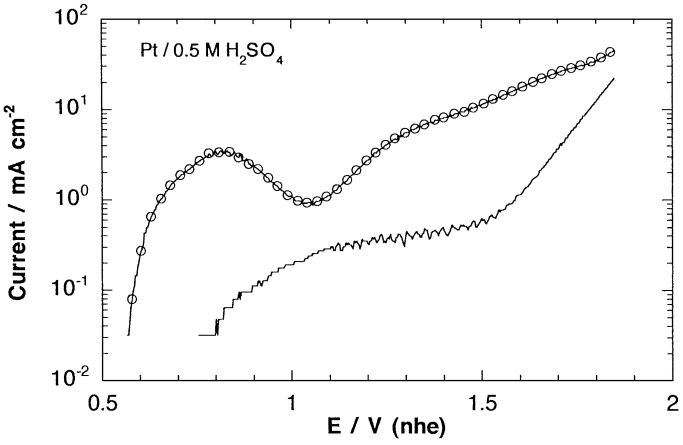

FIG. 4. Current–potential semilogaritmic plots for water oxidation (solid lines) and CH_3OH (1 M) oxidation (open circles) in 0.5 M H_2SO_4 on a Pt electrode. Scanning was from negative to positive potentials at a rate of 5 mV/s.

in powder form as a complement to the measurement performed on the thin layer (cf. Fig. 3a). The molecular oxygen reduction process is also contrasted. It is clearly observed that powder particles embedded in the Nafion matrix deposited on GC electrodes deliver significant signals as compared to the massif electrodes (seen above 1.5 V/nhe, the signals at lower potentials simply refer to the background gas concentration).

Furthermore, it is possible to observe that oxygen and CO_2 evolved on the RuO_2 particles and on the GC substrate, respectively. The CO_2 mass signal from the GC substrate, in the absence of deuterated methanol, is not shown in Fig. 5, due to the restricted applied anodic potential span. The addition of CD_3OD (1 M) favours the CO_2 production (about 1.4 V/nhe) on the RuO_2 particles, resulting in the suppression of water oxidation.

Not all ruthenium-containing compounds are electrocatalysts for the molecular oxygen reduction in acid. Catalytic activity increases in the series RuS_2, $RuSe_2$, and $RuTe_2$. However, it is always below that of the novel compound $Ru_{1-x}Mo_xSeO_z$. The lower extreme case corresponds to RuO_2, as illustrated in Fig. 5. Notice the slight decrease of O_2 (m/e = 32) signal at a potential more negative than 0.15 V/nhe. It is also observed that its low electrocatalytic activity is not perturbed by the presence of deuterated methanol; i.e., there is no formation of CO_2 in the potential span explored negative to 1.5 V/nhe. Furthermore, it is also visible that the current–potential characteristic reflects the oxygen reduction (upper curve) as well as the hydrogen evolution (bottom curve).

4. DISCUSSION

The presented experimental results clearly show that the ruthenium-based electrocatalysts, which allow electron transfer via ruthenium-centred interfacial coordination mechanisms, are all very reactive with water. At the same time, they show little sensitivity for the electrooxidation of methanol. This is in contrast with platinum electrodes, where the reactivity with water is quite low and occurs at a quite high electrode potential while the ability for methanol oxidation is very high.

The fact that oxygen can evolve from water without significant parallel oxidation of methanol, which has a drastically lower oxidation potential, as in the case of RuS_2 or RuO_2, clearly shows that kinetic parameters are involved. The high density of Ru-d states responsible for the

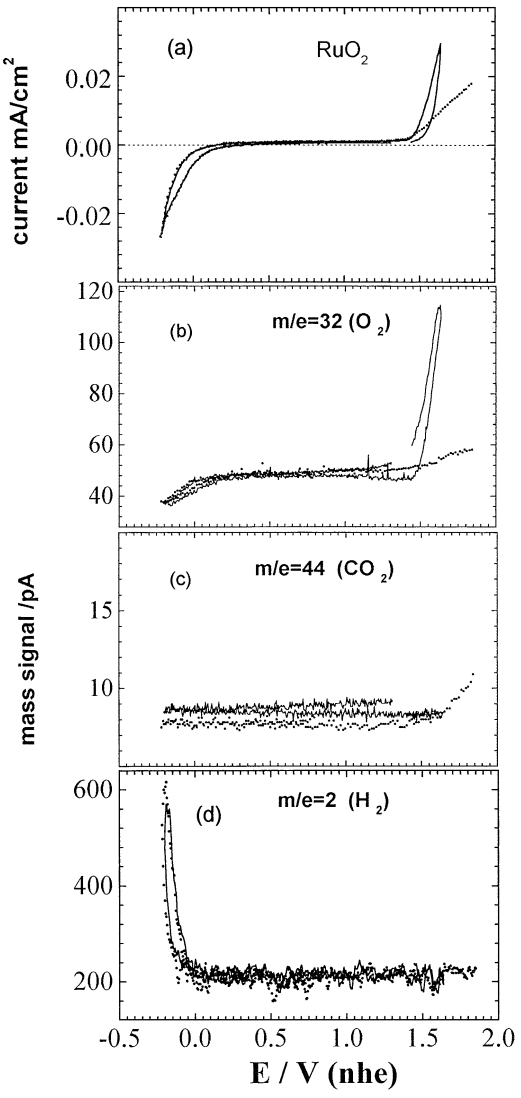

FIG. 5. (a) Current–potential and (b–d) mass signals–potential characteristics for competitive water oxidation and oxygen reduction (solid lines) and competitive water oxidation, oxygen reduction, and methanol oxidation (dotted lines) on Nafion-embedded RuO_2 particles deposited onto a GC substrate in oxygen-saturated 0.5 M H_2SO_4. The molecular oxygen reduction process is clearly contrasted in (b). The cyclic potential scanning rate was made at 5 mV/s.

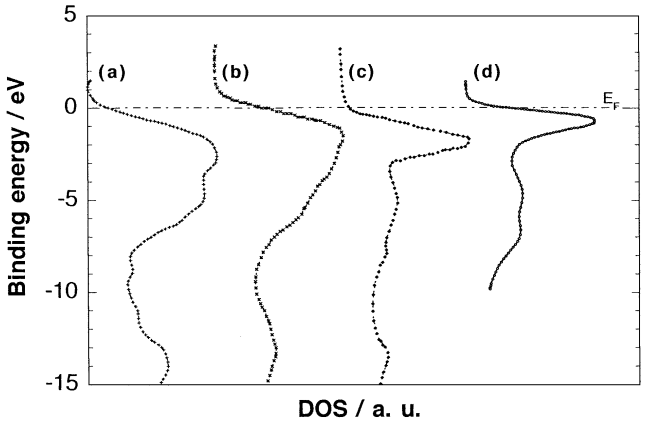

FIG. 6. XPS-photoemision valence band spectra of (a) $Mo_4Ru_2Se_8$, (b) $RuTe_2$, (c) RuS_2, and (d) RuO_2. The data in (a), (b and c), and (d) were adapted from Refs. (26), (22), and (27), respectively. For the sake of comparison, the density of states (DOS) of each spectrum was normalised.

reactivity with water, which becomes involved in Ru-water complexes at a low positive electrode potential, is apparently responsible for the observed selectivity. Sterical factors, e.g., a hindered access of methanol to catalytic centres, can, on the other hand, be excluded due to the structural variety of Ru complexes (pyrite in RuX_2, X = S, Te; rutile in RuO_2; unknown in $Ru_{1-x}Mo_xSeO_z$), which allow for this phenomenon of selectivity. At the Ru-containing compounds/water interface, a displacement of water molecules is not expected since outer-sphere electron transfer shows that electrons can be tunnelled (24). The reason for selectivity must be searched for in the co-ordination chemically determined preference of the Ru-based electrocatalysts for the reaction with water. Methanol molecules have thus a strongly reduced chance to compete for positive electronic charges.

Since Pt electrodes also provide d-metal-centred electrocatalytic pathways, it has to be asked why the investigated Ru-based electrode materials are supporting an improved electrocatalytic mechanism. The primary difference between Pt- and Ru-containing compounds resides in the competition of molecules (water or organics) to be adsorbed onto either the metallic or the oxide layer of such compounds. As supported by the results depicted in Fig. 4, one sees that a competition between methanol and water discharge occurs (both processes being performed between 0.8 and 1.5 V). Reactivity of organics onto other oxides, such as TiO_2, has been reported (25). Here, photogenerated holes favour the formation of radical OH° species, which are able to oxidise organics in an unselective manner. A review of past research (11) puts in relief the catalytic advantages of high concentrations of d-states, which are provided by the investigated semiconducting transition metal compounds. While d-states on metallic electrodes are distributed over a wide energy range, a similar number of d-states is concentrated in a narrow energy region (0–3 eV below the Fermi level, E_F) in compounds like $Mo_4Ru_2Se_8$, RuX_2, (X = S, Te); see Fig. 6. RuO_2, which has an intermediate density of states, is not an excellent O_2-reduction electrocatalyst. What seems to be needed for a selective oxygen electrode (methanol insensitive) is a Ru-based catalyst with exceptionally high d-state density, which catalytically supports the interaction with water species to the extent that methanol oxidation cannot kinetically compete.

5. CONCLUSION

The catalytic selectivity encountered with Ru-based d-band catalysts is essentially the competition of two different electron transfer mechanisms, electron transfer based on strong coordinative interactions and electron transfer based on weak interactions. Our results have shown that the further development of selectivity will imply the search for materials with even more pronounced d-state density distributions near the Fermi level of the electrocatalyst.

REFERENCES

1. Hwan Jung, D., Hyeong Lee, C., Soo Kim, C., and Ryul Shin, D., *J. Power Sources* **71**, 169 (1998).
2. Hogarth, M. P., and Hards, G. A., *Platinum Met. Rev.* **40**, 150 (1996).
3. Savadogo, O., *J. New Mater. Electrochem. Syst.* **1**, 47 (1998).
4. Chun, Y.-G., Kim, C.-S., Peck, D. H., and Shin, D.-R., *J. Power Sources* **71**, 174 (1998).
5. Alonso-Vante, N., and Tributsch, H., *Nature* **323**, 431 (1986).
6. Alonso-Vante, N., Schubert, B., Tributsch, H., and Perrin, A., *J. Catal.* **112**, 384 (1988).
7. Alonso-Vante, N., Schubert, B., and Tributsch, H., *Mater. Chem. Phys.* **22**, 281 (1989).
8. Alonso-Vante, N., *J. Chim. Phys.* **93**, 702 (1996).
9. Solorza, O., Ellmer, K., Giersig, M., and Alonso-Vante, N., *Electrochim. Acta* **39**, 1647 (1994).
10. Alonso-Vante, N., Tributsch, H., and Solorza-Feria, O., *Electrochim. Acta* **40**, 567 (1995).
11. Alonso-Vante, N., and Tributsch, H., *in* "Electrochemistry of Novel Materials" (J. Lipkowski and Ph. Ross, Eds.), Vol III, p. 1. VCH, New York, 1994.
12. Büker, K., Alonso-Vante, N., and Tributsch, H., *Ber. Bunsenges. Phys. Chem.* **100**, 1808 (1996).
13. Ennaoui, A., Fiechter, S., Pettenkofer, Ch., Alonso-Vante, N., Büker, K., Bronold, M., Höpfner, Ch., and Tributsch, H., *Sol. Energy Mater. Solar Cells* **29**, 289 (1993).
14. Seeliger, W., Troughton, G. L., Alonso-Vante, N., and Tributsch, H., *J. Electrochem. Soc.* **142**, L166 (1995).
15. Kötz, R., and Stucki, S., *Electrochim. Acta* **31**, 1311 (1986).
16. Bogdanoff, P., and Alonso-Vante, N., *Ber. Bunsenges. Phys. Chem.* **97**, 940 (1993).
17. Bogdanoff, P., Friebe, P., and Alonso-Vante, N., *J. Electrochem. Soc.* **145**, 576 (1998).
18. Iwasita, T., Nart, F. C., Lopez, B., and Vielstich, W., *Electrochim. Acta* **37**, 2361 (1992).
19. Meli, G., Leger, J. M., Lamy, C., and Durand, R., *J. Appl. Electrochem.* **23**, 197 (1993).
20. Wasmus, S., Wang, J. T., and Savinell, R. F., *J. Electrochem. Soc.* **142**, 3825 (1995).

21. Alonso-Vante, N., *in* "Proceedings, 1st International Symposium for New Materials for Fuel Cells Systems" (O. Savadogo, P. R. Roberge, and T. N. Veziroglu, Eds.), p. 658. École Polytechnique Montréal, 1995.
22. Trassatti, S., *in* "Electrochemistry of Novel Materials" (J. Lipkowski and Ph. Ross, Eds.), Vol. III, p. 207. VCH Publishers, New York, 1994.
23. Kühne, H.-M., Jaegermann, W., and Tributsch, H., *Chem. Phys. Lett.* **112**, 160 (1984).
24. Morrison, S. R., "Electrochemistry at Semiconductor and Oxidized Metal Electrodes." Plenum, New York, 1980.
25. Hoffmann, M. R., Martin, S. T., Choi, W. Y., and Bahnemann, D. W., *Chem. Rev.* **95**, 69 (1995).
26. Jaegermann, W., Pettenkofer, Ch., Alonso-Vante, N., Schwarzlose, Th., and Tributsch, H., *Ber. Bunsenges. Phys. Chem.* **94**, 513 (1994).
27. Riga, J., Tenret-Noel, C., Pireaux, J. J., Caudano, R., and Verbist, J. J., *Phys. Scr.* **16**, 351 (1977).